

See discussions, stats, and author profiles for this publication at: <https://www.researchgate.net/publication/231171861>

Channel Flow Cell for Attenuated Total Reflection Fourier Transform Infrared Spectroelectrochemistry

ARTICLE *in* ANALYTICAL CHEMISTRY · NOVEMBER 1995

Impact Factor: 5.64 · DOI: 10.1021/ac00117a033

CITATIONS

11

READS

20

5 AUTHORS, INCLUDING:



Yuriy Tolmachev

Ftorion

69 PUBLICATIONS 1,014 CITATIONS

SEE PROFILE

Channel Flow Cell for Attenuated Total Reflection Fourier Transform Infrared Spectroelectrochemistry

Rachael Barbour, Zhenghao Wang, In Tae Bae, Yuriy V. Tolmachev, and Daniel A. Scherson*

Department of Chemistry, Case Western Reserve University, Cleveland, Ohio 44106-7078

A channel-type spectroelectrochemical cell is described for the acquisition of potential difference (PD) attenuated total reflection Fourier transform infrared (ATR-FT-IR) spectroscopy of solution phase species generated at an electrode surface under conditions of well-defined laminar flow. The capabilities of the cell have been assessed using the reduction of bisulfite (2 M) in a weakly acidic (pH = 5.25), unbuffered, aqueous electrolyte as a model system. The PD ATR-FT-IR spectrum obtained at -0.85 V vs SCE, a potential negative enough for the reduction of HSO_3^- to proceed, compared to the spectrum recorded at a potential at which no reaction occurs (0.0 V vs SCE) as a reference, was dominated by negative- and positive-pointing contributions due to the reactant, bisulfite, and the predominant product, dithionite, respectively. Also identified in the spectrum was sulfite, which is produced by the dissociation of bisulfite induced by the increase in the pH of the medium during the reduction reaction. Theoretical aspects regarding the quantitative analysis of these data are briefly discussed.

Considerable progress has been made in this laboratory toward the development of in situ optical spectroscopic techniques in the presence of convective flow.¹⁻⁴ Attention has been centered on the coupling of UV-vis spectroscopy with rotating disk (RDE)¹⁻³ and channel-type (CE) electrodes⁴ to monitor the integrated concentration profile of solution phase species. In the first case, a beam of light is reflected off the surface of the RDE at near normal incidence, whereas for the CE, the spectrum is collected in the transmission mode through the solution past the electrode surface. More recently, UV-vis spectroscopy was employed to map the flow in a CE cell.⁵ The results of the latter investigation showed that, under steady state, diffusion-limited conditions, the absorbance measured along an axis normal to the electrode surface (y), at a fixed distance from the electrode downstream edge (x_2), denoted as $A_y(x_2)$, is invariant across the width of the electrode along the full length of the channel. In addition, it was found that $A_y(x_2)$ as a function of x_2 matches the theoretical predictions of the *standard* formalism,⁶ without the introduction of any adjustable parameters. Prompted by the close-to-ideal flow

pattern developed within this CE arrangement, the same cell used for the UV-vis experiments was modified to probe the solution past the electrode surface with attenuated total reflection (ATR) Fourier transform infrared (FT-IR) spectroscopy. This approach makes it, in principle, possible to take advantage of the high specificity of IR spectroscopy for the identification of solution phase products, and possibly relatively stable intermediates, formed at electrode surfaces as a function of the applied potential and other operating conditions.

This note describes the cell employed in these infrared studies and provides the first illustration of the use of ATR-FT-IR for the detection and identification of solution phase products of an electrochemical reaction under well-defined conditions of laminar flow.

EXPERIMENTAL SECTION

Spectroelectrochemical Channel Cell. The CE-type cell designed for in situ UV-vis spectroscopic measurements and described in an earlier paper⁵ (width, $a = 0.9$ cm; height, $2h = 0.11$ cm) was modified to accept a parallelepiped-type ZnSe internal reflection element (IRE, $50 \times 20 \times 3$ mm, 45° , International Crystal), placed adjacent to, and forming a common plane with, the Au working electrode (WE, length, $l = 0.5$ cm; width, $w = 0.6$ cm) cast in Kel-F (see lower section of Figure 1). As indicated in the figure, the long axis of the IRE was aligned normal to the direction of fluid flow. Contributions to the IR signal originating from sections of the channel outside the area defined by the electrode width downstream from the electrode edge (and, therefore, unaffected by the electrochemical reactions) were eliminated by sputtering a thick gold layer onto the large face of the prism (see Figure 1). The back side of the IRE was also coated with a thick layer of gold to avoid other artifactual effects. A saturated calomel electrode (SCE) and a gold piece cast in Kel-F placed downstream from the Kel-F-cast Au WE on the opposite side of the channel were used as reference and counter electrodes, respectively (see upper section of Figure 1).

Instrumentation. All FT-IR spectra were acquired in an IBM IR-98 equipped with a liquid nitrogen-cooled MCT detector at 4 cm^{-1} resolution (zero-filling factor, 2) with the cell mounted on a custom-made reflection absorption attachment. The potential of the electrode was controlled with a PAR Model 173 potentiostat and a PAR Model 175 Universal programmer. The pumping system employed in these studies was the same as that reported elsewhere.^{4,5}

(1) Zhao, M.; Scherson, D. A. *Anal. Chem.* **1992**, *64*, 3064.
(2) Zhao, M.; Scherson, D. A. *J. Electrochem. Soc.* **1993**, *140*, 1671.
(3) Zhao, M.; Scherson, D. A. *J. Electrochem. Soc.* **1993**, *140*, 2877.
(4) Wang, Z.; Zhao, M.; Scherson, D. A. *Anal. Chem.* **1994**, *66*, 4560.
(5) Wang, Z.; Scherson, D. A. *J. Electrochem. Soc.*, submitted.

(6) (a) Albery, W. J.; Coles, B. A.; Couper, A. M. *J. Electroanal. Chem.* **1975**, *65*, 901. (b) Coles, B. A.; Compton, R. G. *J. Electroanal. Chem.* **1983**, *144*, 87.

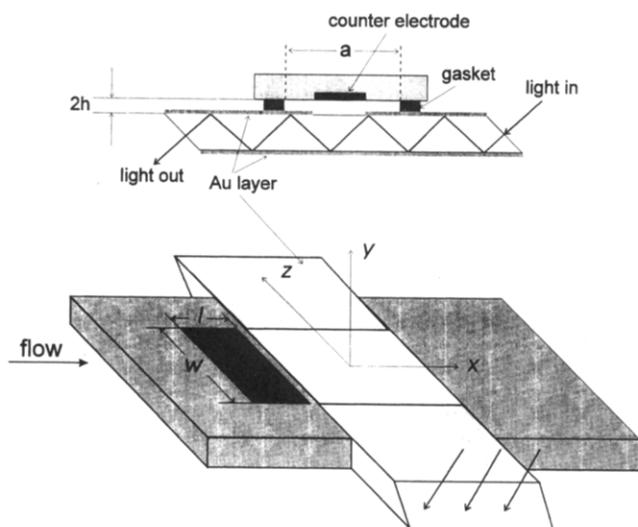


Figure 1. Schematic diagram of a channel-type spectroelectrochemical cell for ATR-FT-IR measurements of solution phase electrogenerated species under well-defined conditions of laminar flow (lower figure). For the sake of clarity, some of the cell components have been omitted. l and w are the length and width of the electrode, respectively. A partial view of the cell along the direction of fluid flow is shown in the upper figure, where $2h$ is the full height of the channel cell. The darker area in the center of the component directly above the gasket represents the counter electrode cast in Kel-F.

Electrochemical Standardization of the Spectroelectrochemical CE-Type Cell. After assembly, and prior to the spectroelectrochemical experiments, the proper operation of the CE-type cell was tested with a 10 mM $\text{Fe}(\text{NH}_4)_2\text{SO}_4$ solution in 0.1 M H_2SO_4 . A plot of the diffusion limited current vs $V^{1/3}$, where V is the flow rate (in mL/s), was linear in the range $0.07 < V < 2.0$ mL/s (slope, $S = 0.73 \pm 0.02 \text{ mA}(\text{s/mL})^{1/3}$; intercept, 0.007; correlation, $R = 0.9993$). The magnitude of S was found to be in excellent agreement with that calculated on the basis of the dimensions of the channel and the electrode (see above) and the diffusion coefficient of the ferrous species evaluated from independent rotating disk measurements ($5.3 \times 10^{-6} \text{ cm}^2/\text{s}$), i.e., $S = 0.71 \text{ mA}(\text{s/mL})^{1/3}$.

ATR-FT-IR Spectroelectrochemical Arrangement. After thorough rinsing, the cell was mounted on the reflection absorption attachment and placed in the sample compartment (SC) of the spectrometer. Two openings on the lid of the SC were used to house the inlet and outlet solution feedthroughs to the cell. During spectral acquisition, the SC was purged with nitrogen to minimize spectral contributions due to water vapor and carbon dioxide.

In Situ ATR-FT-IR Measurements under Forced Convection. Possible spectral artifacts derived from the continuous flow of liquid through the cell were examined by ratioing two sets of 100 coadded scans obtained in sequence using a 0.22 M bisulfite solution in an aqueous phosphate buffer. The results obtained revealed no differences between ratioed spectra recorded under forced convection and stagnant conditions, indicating that the operation of the pump does not affect to any significant extent the spectral quality. Following these measurements, the solution reservoir, including the cell, was filled with a 2 M NaHSO_3 solution (Fisher, ACS analyzed) prepared with ultrapure water obtained from a modified Gilmont distillation system and adjusted to pH = 5.25 with concentrated NaOH. Spectra were recorded with the electrode polarized at a potential $E_{\text{ref}} = 0.0 \text{ V}$ vs SCE, at which no

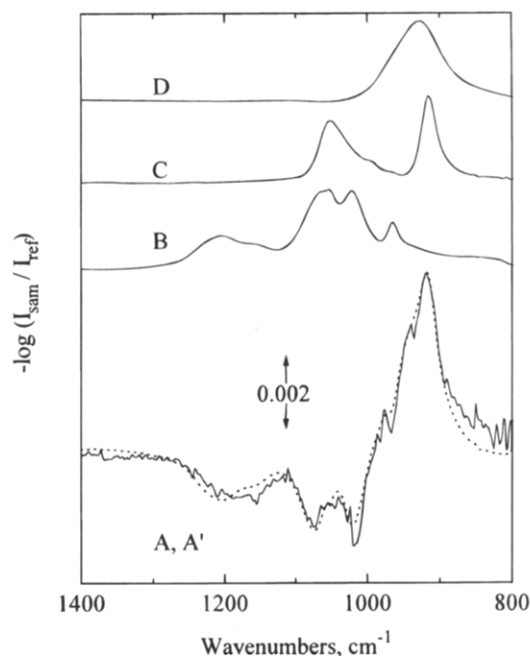


Figure 2. Curve A (solid line): Potential difference ATR-FT-IR spectrum for the reduction of bisulfite ion in an aqueous solution at pH = 5.25, obtained using the *sequential* method (see text for details) with $E_{\text{ref}} = 0.0 \text{ V}$ and $E_{\text{sam}} = -0.85 \text{ V}$ vs SCE. Flow rate, $V = 0.07 \text{ mL/s}$. Curve B: Solution phase spectrum of a 2 M bisulfite ion solution ratioed against water. Curve C: Solution phase spectrum of a 0.5 M dithionite solution in 2 M bisulfite solution ratioed against a 2 M bisulfite solution. Curve D: Solution phase spectrum of a 0.5 M sulfite solution ratioed against water. Curve A' (dotted line) was obtained by a combination of spectral contributions due to bisulfite ($0.0073 \times$ curve B), dithionite ($0.011 \times$ curve C), and sulfite ($0.019 \times$ curve D) (see text for details).

reaction takes place, and at $E_{\text{sam}} = -0.85 \text{ V}$ vs SCE, at which the reduction of bisulfite proceeds at significant rates, for flow rates in the range 0.07 – 0.8 mL/s . The spectral collection was effected either by coadding 1000 interferometric scans *sequentially*, first at E_{sam} and then at E_{ref} , or by acquiring 10 scans alternately at E_{sam} and E_{ref} , with a 20 s time delay after each potential *switch* (by a step) to allow the concentration profile to achieve steady state. A total of 1000 scans were recorded at each potential, which were then coadded and stored in the computer for further processing. In both cases, the results are displayed in the form $-\log I_{\text{sam}}/I_{\text{ref}}$ vs wavenumber, where I_{sam} and I_{ref} represent single beam spectra obtained at the sampling E_{sam} and reference E_{ref} potentials, respectively.

ATR-FT-IR Spectra of Reference Materials. ATR-FT-IR spectra of 2 M NaHSO_3 (curve B, Figure 2) and 0.4 M Na_2SO_3 (curve C, Figure 2), ratioed against water, and 0.5 M $\text{Na}_2\text{S}_2\text{O}_4$ (sodium dithionite) in 2 M NaHSO_3 , ratioed against 2 M NaHSO_3 (curve D, Figure 2), were collected under stagnant conditions using an uncoated ZnSe crystal. These were used as references for the analysis of potential difference (PD) ATR-FT-IR spectra obtained in situ.

RESULTS AND DISCUSSION

Reduction of Bisulfite Ion in a Weakly Acidic, Unbuffered, Aqueous Electrolyte. A typical PD ATR-FT-IR spectrum for the reduction of a 2 M HSO_3^- , unbuffered, aqueous solution (pH = 5.25) on a gold electrode in a channel-type cell (flow rate, $V = 0.07 \text{ mL/s}$), obtained using the *sequential* method ($E_{\text{ref}} = 0.0 \text{ V}$

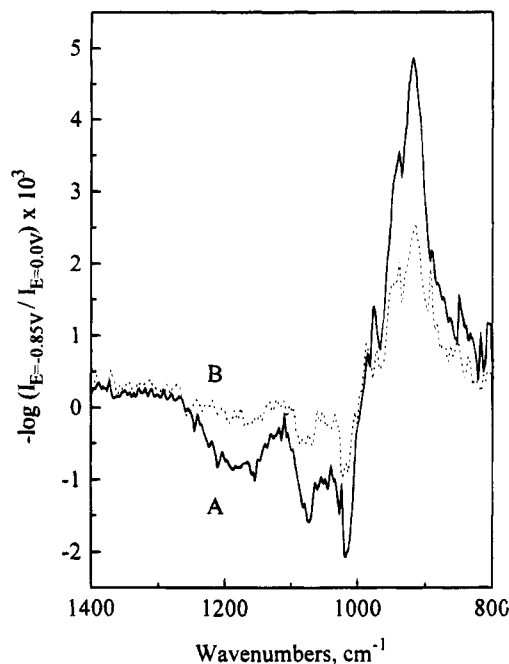


Figure 3. Comparison between PD-ATR-FT-IR spectra obtained in the *sequential* mode under the experimental conditions specified for curve A in Figure 2 for flow rates $V = 0.07$ (curve A) and 0.35 mL/s (curve B).

and $E_{\text{sam}} = -0.85$ V vs SCE), is shown in curve A (solid line) of Figure 2. As may be expected on the basis of hydrodynamic considerations, an increase in V gives rise to a decrease in the magnitude of the spectral features, as the differences in the solution composition become smaller with increased convection. This effect is illustrated in Figure 3, which compares spectra obtained for $V = 0.07$ (curve A) and 0.35 mL/s (curve B).

Only a slight improvement in signal-to-noise was observed for measurements performed using the *switching* instead of the *sequential* mode (not shown), indicating that effects due to long-term drifts are not very significant.

Spectral Assignment. The positions of the negative- and positive-pointing bands of typical PD ATR-FT-IR recorded in these experiments (see solid line, curve A, Figure 2) are in agreement with those of bisulfite and dithionite ($\text{S}_2\text{O}_4^{2-}$) shown in curves B and C in the same figure. This indicates that $\text{S}_2\text{O}_4^{2-}$ is one of the predominant products of the reduction of HSO_3^- on Au under the experimental conditions selected for these studies.

Careful inspection of these curves, however, revealed that the feature attributed to $\text{S}_2\text{O}_4^{2-}$ in the PD ATR-FT-IR spectra (918 cm^{-1}) is much broader than that of pure $\text{S}_2\text{O}_4^{2-}$ in the same medium (see curve C in this figure). The most likely explanation for this effect may be due to the presence of SO_3^{2-} , for which the spectrum shows a band centered at 927 cm^{-1} (see curve D in this figure). Sulfite can be generated via acid-base equilibrium due to an increase in pH derived from the reduction of HSO_3^- on the electrode surface in this unbuffered media. In fact, the experimental PD ATR-FT-IR spectrum (see curve A, Figure 2) could be successfully resolved in terms of the sum of negative-pointing bisulfite ($0.0073 \times$ curve B) and positive-pointing dithionite ($0.011 \times$ curve C) and sulfite ($0.019 \times$ curve D) contributions, to yield curve A' (dotted line) in this figure. Each of the numerical factors in parentheses can be multiplied by the specific concentration of the reference spectrum to obtain the *average* concentration

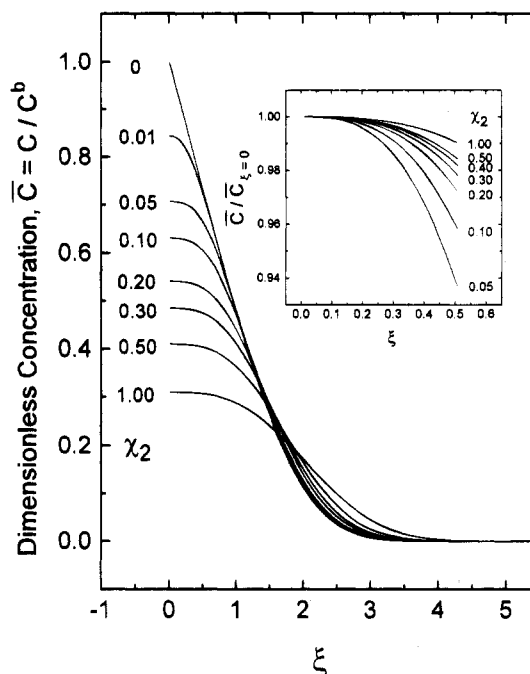


Figure 4. Plots of the dimensionless concentration of a product ($\bar{c} = c/c^b$), generated at the surface of an electrode in a channel under steady state, diffusion-limited conditions, as a function of the dimensionless distance normal to the plane of electrode ξ past the electrode surface. The values next to each of the curves represent dimensionless distances from the downstream edge of the electrode along the direction of fluid flow, χ_2 . The inset shows plots of the relative changes in the surface concentration of the product ($\bar{c}/\bar{c}_{\xi=0} \equiv c/c_{\xi=0}$) as a function of the distance from the surface, over the range $0 < \xi < 0.5$, for different values of χ_2 .

of each of the species generated or consumed by the electrochemical reaction.

Theoretical Considerations. Considerable insight into a quantitative interpretation of PD ATR-FT-IR spectra of the type shown in curves A of Figures 2 and 3 can be gained on the basis of an analysis of the concentration profile past the electrode surface along x and y (see Figure 1). Figure 4 shows plots of the steady state, dimensionless concentration ($\bar{c}_0 = c/c^b$) profile of a product generated at the surface of an electrode under diffusion-limited conditions along a dimensionless axis normal to the electrode surface, $\xi = (3V/2ah^2D_0)^{1/3}y$, where c^b is the bulk concentration of the reactant, a the channel width, h the half-cell thickness (cm), and D_0 the diffusion coefficient of the product (cm^2/s). These curves were calculated by a numerical integration of the *standard* governing differential equation,⁶ for various values of the dimensionless variable $\chi_2 = x_2/l$, where x_2 is the actual distance along x measured from the downstream edge of the electrode. Except for $\chi_2 = 0$, the downstream electrode edge, the profile along ξ (or y) is characterized by a fairly flat region close to the channel surface ξ , i.e., $y = 0$, followed by a linear section, which decays exponentially into the bulk of the solution. A detailed inspection of the behavior close to the surface shows that for values of $x_2 > l/10$, the actual product concentration in the region $0 < \chi < 0.5$ differs by no more than 5% from its value on the surface (see inset in Figure 4). This observation is of much significance, as for reasonable values for the parameters involved, e.g., $h = 0.055$ cm, $a = 0.9$ cm, $D_0 = 5 \times 10^{-6}$ cm^2/s , $l = 0.5$ cm, and for flow rates in the range $V = 0.1$ – 1 mL/s, $\xi = 0.5$ corresponds to actual distances from 18 down to 8 μm , and

therefore longer than the theoretical penetration depth of the IR radiation for the ZnSe/solution interface in the fingerprint region (3–5 μm). Since the concentration profile at a fixed χ_2 is invariant along the width of the electrode, the region probed by the FT-IR beam displays only χ_2 dependence.⁵ This is particularly convenient, as $c(\chi_2, 0)$, the surface concentration of the product past the electrode surface under diffusion-limited conditions (see Figure 4 for $\xi = 0$), can be expressed in analytic form based on the integral formalism introduced originally by Lighthill.⁷

The application of chemometric techniques, such as those implemented by Bennett and co-workers⁸ for the rigorous analysis of ex situ ATR-FT-IR aqueous mixtures of sulfur–oxygen anions, may be expected to provide the necessary information to establish quantitatively reaction rates and mechanisms as a function of the applied potential for a wide variety of electrode processes. It should be pointed out that, despite the high concentration of bisulfite in the solution, the signals observed are relatively small.

(7) Lighthill, M. J. *Proc. R. Soc. London* **1950**, *A202*, 359.

(8) Holman, D. A.; Thompson, A. W.; Bennett, D. W.; Otvos, J. D. *Anal. Chem.* **1994**, *66*, 1378.

This is due to the fact that under the conditions selected for these experiments, the current is well below its diffusion-limited value for the reduction of bisulfite, and therefore, the amount of product generated is rather small. Furthermore, the dimensions of the electrode and the cell used in these studies enable only one or two reflections at the IRE element/solution interface. Both of these factors should be carefully considered in the search of strategies for the further optimization of this type of channel cell in situ ATR-FT-IR experiments.

ACKNOWLEDGMENT

This work was supported by ARPA Grant No. N-000-14-92-J-1848. Valuable discussions with Prof. Bennett are gratefully acknowledged.

Received for review May 8, 1995. Accepted August 15, 1995.*

AC950436A

* Abstract published in *Advance ACS Abstracts*, September 15, 1995.